C_3-symmetric ferrichrome-mimicking Fe^{3+}-complexes containing the 1-hydroxypyrimidinone Fe^{3+}-binding moieties based on α-cyclodextrin: helicities in solvent environments

Takeshi Masuda, Jun-ichiro Hayashi and Seizo Tamagaki *

Department of Bioapplied Chemistry, Faculty of Engineering, Osaka City University, 3-3-138 Sugimoto, Sumiyoshi-ku, Osaka 558-8585, Japan

Received (in Cambridge, UK) 24th May 1999, Accepted 26th October 1999

Two homologous C_3-symmetric ferrichrome mimics, *La* and *Lb*, equipped with three 1-hydroxypyrimidinone terminals for receiving an Fe^{3+} ion have been designed and synthesized; the side chains of *La* and *Lb*, which include dimethylene and pentamethylene spacers, respectively, are anchored to the narrower rim of the α-cyclodextrin framework through an amide linkage. The 1 : 1 Fe^{3+}-complexes of *La* and *Lb* provide strong circular dichroic exciton coupling of negative and positive signs at 480 nm, showing Δ- and Λ-helices, respectively, in polar aprotic solvents such as dimethylformamide and dimethyl sulfoxide. The magnitude of the signals increases with the increasing hydrogen-bond accepting ability of the solvent. It is inferred, therefore, that hydrogen-bonding interactions of the linker amide N–H groups with the solvent play a primary role in inducing a helicity within aprotic solvents. The mechanisms of the helicity inductions are discussed.

Meanwhile, the signals for *La* are still negative, but weak in alcohols and water. However, the signal sign for *Lb* having the relatively flexible spacers depends on the nature of alcohols, and no CD signal was observed in water.

Naturally occurring siderophores such as ferrichrome and enterobactin are tripodal chiral Fe^{3+}-specific chelating agents and their production is required for solubilization and transportation of Fe^{3+} ions in microorganisms[1] in which the Fe^{3+} ion is embedded in the octahedral cavity of three bidentate ligands on the side-chains. Iron chelation is also important in therapeutic treatments of a human genetic disease, Cooley's anemia.[2] Many synthetic or natural siderophores have been tested for the therapic treatments, and desferrioxamine B, a simple linear ferrichrome-mimicking compound, has been developed for practical utility.

Among various ferrichrome mimics, tripodal types of compounds in particular have attracted our attention thus far, because covalently linking the ligand chains in a C_3-symmetric way to a common anchor would reduce the number of possible complexed species and enable us to unequivocally elucidate the most feasible conformation of the complex.[3] Recent publications on tripodal Fe^{3+} complexes[4] prompted us to design another type of tripodal complex and to implicate the mechanism of the induced helicity; as part of our continuing research we have recently reported C_3-symmetric tripodal mimics constructed on the narrower face of the rigid α-cyclodextrin framework (α-CyD) instead of a cyclic lactone ring in the natural ferrichrome, and shown that the linking of three monohydroxamate side-chains to the α-CyD results in a twisting of the octahedral chromophore around the Fe^{3+} ion to preferentially produce a Δ-*cis*,*cis* complex with a right handed helicity (observed CD amplitude/mdeg: −26 (H_2O) < −16 (MeOH) < −8 (acetonitrile) < −2 (dimethyl sulfoxide, no complexation) < −1 (pyridine, no complexation)),[5] and the extent of the right-handedness decreases with decreasing solvent polarity and/or hydrogen bond donating ability of the solvent. The chiral cyclodextrin skeleton is an origin of induced helical chirality around the Fe^{3+} ion in an octahedral cavity. Meanwhile, the ligand having bis-hydroxamate side chains (*Lc*, Fig. 1), anticipated to form a triply helical binuclear complex, was found to provide a Δ-*cis*,*cis* complex in water. However, complexation in rather basic aprotic solvents such as pyridine and acetone led to the Λ-*cis*,*cis* complex with absolutely opposite helicity (observed CD amplitude/mdeg: −10 (H_2O) < −3 (MeOH) < 0 (dimethyl sulfoxide, no complexation) < +5 (acetonitrile) < +8 (acetone) < +15 (pyridine)).[6] We have suggested, accordingly, the primary importance of steric repulsion between the hydroxamate carbonyl and linker carbonyl groups and intermolecular hydrogen-bonding with the solvent in enhancing the Λ-helicity.

To provide extensive systematic investigations for these fundamentally interesting concepts, we will report here the synthesis and physico-chemical properties of C_3-symmetric ferrichrome surrogates (*La* and *Lb* in Fig. 1) that are assembled from an α-cyclodextrin as a tripodal anchor and three pendant side chains with 1-hydroxypyrimidinone terminals as an iron binding site.[7] We have now found that the effects of solvent environments on helical chirality substantially differ for the hydroxamate and 1-hydroxypyrimidinone complexes. Helical chirality has currently been a central feature of chemical systems which are involved in a wide variety of biologically and technologically important processes.[8]

Experimental

Materials

Solvents such as alcohols, tetrahydrofuran (THF), acetonitrile (MeCN), acetone (Me_2CO), formamide ($HCONH_2$), dimethylformamide (DMF) and dimethyl sulfoxide (DMSO) were all distilled after drying before use. $Fe_2(NO_3)_2 \cdot 8H_2O$ was purchased from Tokyo Kasei Co. (Tokyo, Japan) and used as received. Ligands *La* and *Lb* were prepared according to Scheme 1. The preparation of the key intermediate **4a**, the very same compound, had been achieved by Katoh *et al.*[9] Therefore, the synthetic procedures for **2a**, **3a**, and **4a** have been omitted here.

4-[5-(Methoxycarbonyl)pentylamino]-1-(benzyloxy)pyrimidin-2(1*H*)-one (2b). 1-Benzyloxy-4-(1,2,4-triazol-1-yl)pyrim-

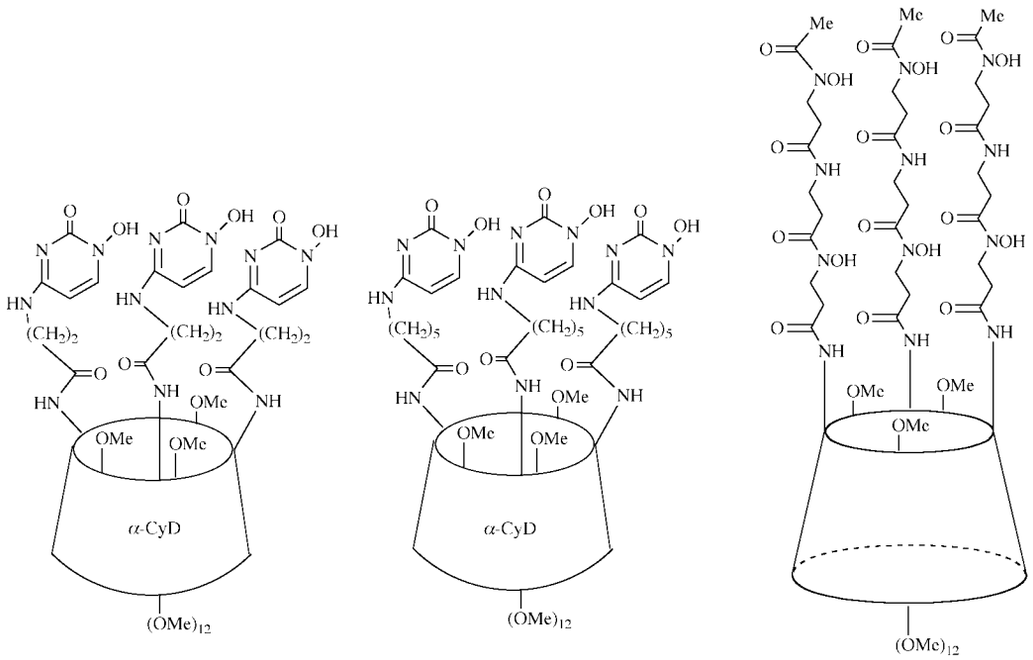

Fig. 1 Chemical structures of ligands.

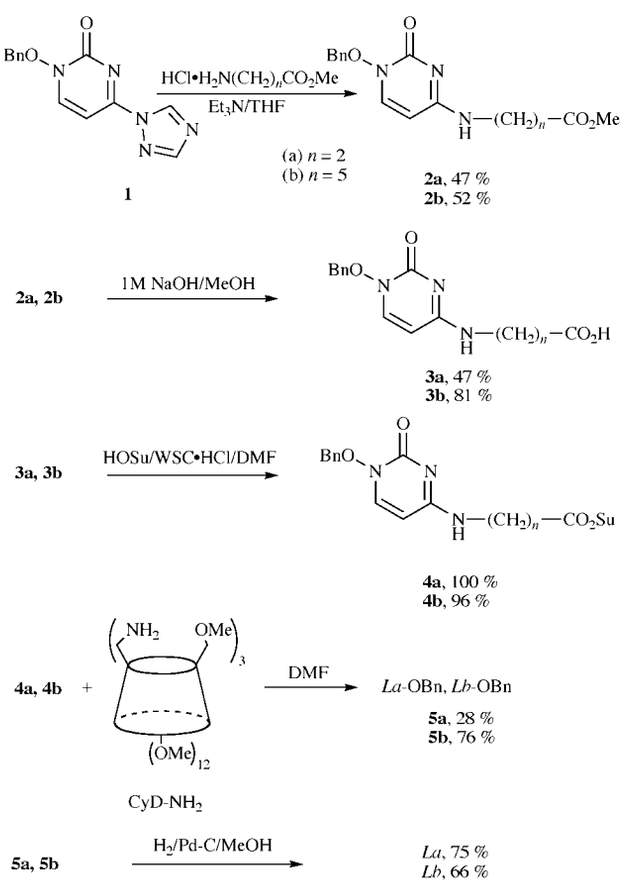

Scheme 1

idin-2(1*H*)-one[10] (**1**, 960 mg, 3.57 mmol) was treated with the HCl salt of methyl 6-aminohexanoate (960 mg, 5.3 mmol) and triethylamine (0.73 mL, 5.3 mmol) in 30 mL of dried THF and stirred at room temperature for 14 h. After addition of 15 mL of water, the mixture was extracted five times with $CHCl_3$.

Evaporation of the solvent and recrystallization of the residue from EtOH gave **2b** (640 mg, 1.86 mmol, 52%): mp 144–145 °C; IR(KBr) 3025, 1672, 1616, 746, 700 cm^{-1}; Anal. Found: C, 62.43; H, 6.88; N, 12.11%. Calcd for $C_{18}H_{23}N_3O_4$: C, 62.59; H, 6.92; N, 12.17%; ^{1}H NMR($CDCl_3$) δ 1.37–1.39 (m, 2H, 3-CH_2), 1.60–1.66 (m, 4H, 2,4-CH_2), 2.32 (t, J = 7.4 Hz, 2H, CH_2CO), 3.22–3.28 (m, 2H, NHCH_2), 3.67 (s, 3H, CH_3O), 5.07 (s, 2H, CH_2Ph), 5.53 (d, J = 7.6 Hz, 1H, N–CH=C*H*), 7.40–7.45 (m, 5H, Ph), 7.56 (d, J = 7.6 Hz, 1H, N–C*H*=CH), 7.73 (s, 1H, NH).

4-[5-(Carboxy)pentylamino]-1-(benzyloxy)pyrimidin-2(1*H*)-one (3b). Into a solution of **2b** (590 mg, 1.7 mmol) in 25 mL of MeOH was added 5 mL of 1 M aq. NaOH solution under cooling, and stirred for 10 h. Removal of the solvent and acidification with 1 M HCl to pH 3 resulted in precipitation of **3b** (460 mg, 1.4 mmol, 81%): mp 192–193 °C; IR(KBr) 3220–2830, 1710, 1645, 750, 700 cm^{-1}; Anal. Found: C, 61.23; H, 6.52; N, 12.38%. Calcd for $C_{17}H_{21}N_3O_4$: C, 61.62; H, 6.39; N, 12.68%; ^{1}H NMR(DMSO-d_6) δ 1.31 (br. t, J = 7 Hz, 2H, 3-CH_2), 1.44–1.56 (m, 4H, 2,4-CH_2), 2.21 (t, J = 7.6 Hz, 2H, CH_2CO), 3.18–3.23 (m, 2H, NHCH_2), 5.07 (s, 2H, CH_2Ph), 5.51 (d, J = 7.6 Hz, 1H, CH), 7.39–7.46 (m, 5H, Ph), 7.56 (d, J = 7.6 Hz, 1H, C*H*=C), 7.70 (br. t, J = 8 Hz, 1H, N*H*).

4-[5-(Carboxy)pentylamino]-1-(benzyloxy)pyrimidin-2(1*H*)-one-*O*-succinimide (4b). 3b (340 mg, 1.02 mmol) and the water-soluble carbodiimide (1-ethyl-3-(3-dimethylaminopropyl)-carbodiimide hydrochloride, WSC, 480 mg, 2.5 mmol) was added into 10 mL of a DMF solution of *N*-hydroxysuccinimide (290 mg, 2.5 mmol) at −10 °C. The solution was kept standing at the same temperature for 1 h and then at room temperature for 14 h. Removal of precipitates and the solvent, followed by addition of water and extraction with $CHCl_3$, eventually gave **4b** (420 mg, 0.98 mmol, 96%): mp 186–189 °C; IR(KBr) 1810, 1780, 1740, 1600, 745, 695 cm^{-1}; Anal. Found: C, 6.23; H, 6.02; N, 12.59%. Calcd for $C_{21}H_{24}N_4O_6$: C, 61.62; H, 6.39; N, 12.68%; ^{1}H NMR(DMSO-d_6) δ 1.38 (br. s, 2H, 3-CH_2), 1.51 (br. s, 2H, 2-CH_2), 1.64 (br. s, 2H, 4-CH_2), 2.67 (br. t, J = 7 Hz, 2H, CH_2CO), 2.81 (s, 4H, OCCH_2CH_2CO), 3.20–3.22 (br. s, 2H, CH_2NH), 5.07 (s, 2H, CH_2Ph), 5.51 (d, J = 7.6 Hz, 1H, N–CH=C*H*), 7.40–7.45 (m, 5H, Ph), 7.56 (d, J = 7.6 Hz, 1H, N–C*H*=CH), 7.73 (s, 1H, N*H*). The product was judged pure enough to proceed to the next step.

***La*-OBn (5a).** Into 6^A,6^C,6^E-triamino-6^A,6^C,6^E-trideoxy-

$2^A,2^B,2^C,2^D,2^E,2^F,3^A,3^B,3^C,3^D,3^E,3^F,6^B,6^D,6^F$-pentadeca-*O*-methyl-α-CyD (CyD-NH_2,[11] 420 mg, 0.36 mmol) dissolved in 60 mL of DMF was added **4a** (500 mg, 1.3 mmol) and the solution was stirred for 1 day at 40 °C. After removal of the solvent, the residue was subjected to column chromatography on silica gel ($CHCl_3$–MeOH 7:1 v/v) and **5a** was obtained in 28% yield (210 mg, 0.1 mmol): mp 165–168 °C; ^{1}H NMR(DMSO-d_6) δ 2.41 (br. s, 6H, CH_2CO), 3.00–3.72 (m, 114H, CyD C–H and H_2O protons), 4.97 (br. s, 6H, CyD C-1 protons), 5.06 (s, 6H, CH_2Ph), 5.58 (d, J = 7.6 Hz, 3H, N–CH=C*H*), 7.39–7.44 (m, 15H, Ph), 7.62 (d, J = 7.2 Hz, 3H, N–C*H*=CH), 7.80 (br. s, 3H, N*H*); MS(FAB$^+$): *m*/*z* 1994 (M + 1) for $C_{93}H_{133}N_{12}O_{36}$.

***Lb*-OBn (5b).** The compound was prepared from **4b** and CyD-NH_2 according to the same method as mentioned above. The product was obtained in 76% yield (350 mg, 0.16 mmol); mp 147–150 °C; ^{1}H NMR(DMSO-d_6) δ 1.29 (br. s, 6H, 3-CH_2), 1.47 (br. s, 12H, 2,4-CH_2), 2.13 (br. s, 6H, CH_2CO), 3.02–3.72 (m, 116H, CyD C-1 protons), 4.96 (br. s, 6H, CyD C-1 protons), 5.06 (s, 6H, CH_2Ph), 5.51 (d, 3H, J = 7.2 Hz, 3H, N–CH=C*H*), 7.39–7.43 (m, 15H, Ph), 7.57 (d, J = 7.2 Hz, 3H, N–C*H*=CH), 7.74 (s, 3H, N*H*); MS(FAB$^+$): *m*/*z* 2121 (M + 1) for $C_{102}H_{150}N_{12}O_{36}$.

Deprotection of the benzyl groups. 10% Pd/C (25 mg) was added into a 20 mL MeOH solution of **5a** (200 mg, 0.096 mmol). A stream of hydrogen gas was bubbled into the mixture for 14 h. After disappearance of the starting compound on a TLC plate, Pd/C was filtered and the solvent was distilled off. Dissolving the residue in a small amount of water and lyophilization afforded *La* in 75% yield: mp 168–170 °C; ^{1}H NMR(DMSO-d_6) δ 2.41 (br. s, 6H, CH_2CO), 3.05–3.67 (m, 147H, CyD and H_2O protons), 4.97 (br. s, 6H, CyD C-1 protons), 5.61 (d, J = 7.6 Hz, 3H, N–CH=C*H*), 7.67–7.82 (m, 6H, NH and N–C*H*=CH); MS(FAB$^-$): *m*/*z* 1721 (M − 1) for $C_{72}H_{113}N_{120}O_{36}$.

Similarly, debenzylation of **5b** gave *Lb* in 75% yield: mp 168–170 °C; ^{1}H NMR(DMSO-d_6) δ 1.23 (br. s, 6H, 3-CH_2), 1.47 (br. s, 12H, 2,4-CH_2), 2.12 (br. s, 6H, CH_2CO), 3.00–3.72 (m, 111H, CyD and H_2O protons), 4.97 (br. s, 6H, CyD C-1 protons), 5.58 (d, J = 7.6 Hz, 3H, N–CH=C*H*), 7.65 (m, 6H, NH and N–C*H*=CH); MS(FAB$^-$): *m*/*z* 1847 (M − 1) for $C_{81}H_{131}N_{12}O_{36}$. No peaks due to the benzyl protons were observed in either case; the NMR spectra of the debenzylated products were identical with those of the corresponding benzylated derivatives except for the lack of benzyl peaks at 5.06 ppm and at 7.4 ppm. TLC of *La* and *Lb* showed a single spot at the starting point, which was colored with Fe^{3+}, indicating that the hydrogenolysis resulted in debenzylation. The products were judged pure enough for titration experiments. Therefore, no further purification was attempted.

Instruments

IR spectra were recorded on a Shimadzu FT-IR 8200 spectrometer. ^{1}H NMR spectra were measured using a Nihondensi Detum α-400 spectrometer operating at 400 MHz. UV–vis and CD spectra were recorded on a Shimadzu UV-2500 PC spectrophotometer and a J-720 circular dichroism spectrophotometer, respectively. The FAB-MS spectra were recorded on a Nihon Bunko JMS-700T spectrometer.

UV–vis and CD titrations

A typical procedure: Titrations were performed in a thermostatted cell holder maintained at 25 °C and the following protocol was typically employed: A stock solution of 54.2 mg *La* in 1 mL of MeOH, a 5 mL stock solution containing 90.9 mg $Fe(NO_3)_3 \cdot 9H_2O$, and a 5 mL stock solution containing 83.9 μL 2,6-lutidine were prepared on the day of the experiment.

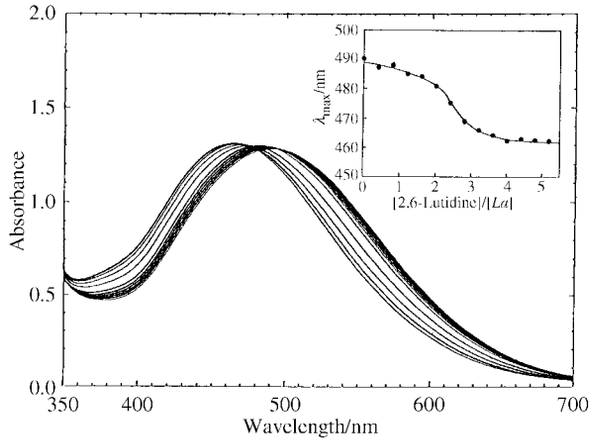

Fig. 2 Changes in UV–vis absorption spectra for the *La*–Fe^{3+} complex in MeOH with various concentrations of 2,6-lutidine. [*La*] = [Fe^{3+}] = 0.3 mM, [2,6-lutidine] = 0–1.56 mM. The inset shows a plot of λ_{max} *versus* [2,6-lutidine]/[*La*].

Stock solutions of 30 μL ligand and 20 μL Fe^{3+} ([L] = [Fe^{3+}] = 0.3 mM) were added into 3 mL of MeOH in a UV cell. The same samples used for UV measurements were also employed for the CD measurements.

Results and discussion

Complexation of *La* with Fe^{3+}

A MeOH solution of an equimolar mixture of *La* and $Fe(NO_3)_3$ afforded a UV–vis spectrum involving a maximum absorption band at 490 nm. The absorption at 490 nm demonstrates the existence of di- and/or tetra-coordinate complexes, but not a hexa-coordinate octahedral complex.[12] Fig. 2 displays the spectra of the MeOH solution in the presence of different concentrations of 2,6-lutidine base. The band maximum shifted with increasing base concentrations eventually getting to 458 nm, which was attributable to the ligand-to-metal charge transfer absorption of the octahedral complex. Thus, to make the reaction go to completion in organic solvents, the addition of a certain amount of base into the system would be required to effectively deprotonate the 1-hydroxy group on the pyrimidinone ring.[4] In fact, as one can see from the inset of Fig. 2, at least four equivalents of the base were needed to attain a constant absorbance at 458 nm. Therefore, UV–vis spectra were measured at several different concentrations of Fe^{3+} in the presence of six equivalents of 2,6-lutidine over the ligand all through this study. The change in absorbance in MeOH with changing molar concentrations of Fe^{3+} at a constant concentration of *La* is shown in Fig. 3 and the inset of Fig. 3 displays a titration plot of the absorbance at 458 nm *versus* Fe^{3+} concentration which has a sharp break point at a 1:1 molar ratio, confirming that the existing single species has a stoichiometric composition of 1 equivalent of Fe^{3+} for 1 equivalent of *La* expected for a 1:1 complex.

CD spectra were also measured at different concentrations of Fe^{3+} in the presence of an excess of 2,6-lutidine. Generally speaking, the spectra all show an exciton coupling-type Cotton effect between the pyrimidinone rings, *i.e.*, a positive band at 400 nm and a negative band at 490 nm (called a negative exciton coupling) and an isodichroic point at approximately 440 nm, which is a region where all the traces converge, demonstrates that either one of two possible conformers (a right-hand helicity, Δ and a left-hand helicity, Λ) should be predominant during the titration in these solvents. Evidently, the chiral template α-CyD provides necessary symmetry conditions for distinguishing between right- and left-handed triple helices. CD spectra of the complex in, for example, MeOH and DMSO solvents are comparatively displayed in Fig. 4a and 4b,

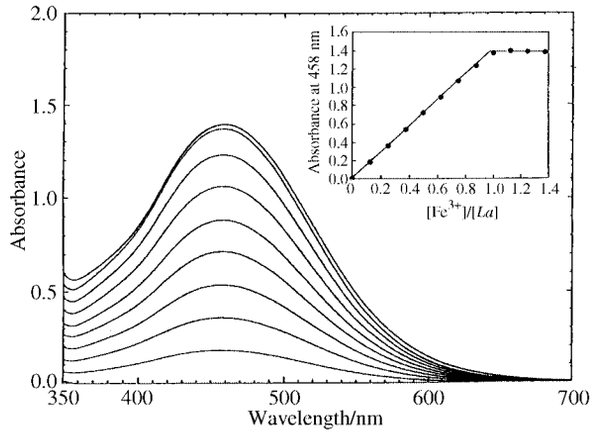

Fig. 3 Changes in UV–vis absorption spectra for the *La*–Fe^{3+} complex in MeOH with altering Fe^{3+} concentrations. [*La*] = 0.3 mM, [2,6-lutidine] = 1.8 mM, [Fe^{3+}] = 0–0.41 mM. The inset shows a variation of absorbance at λ_{max} 458 nm as a function of [Fe^{3+}]/[*La*].

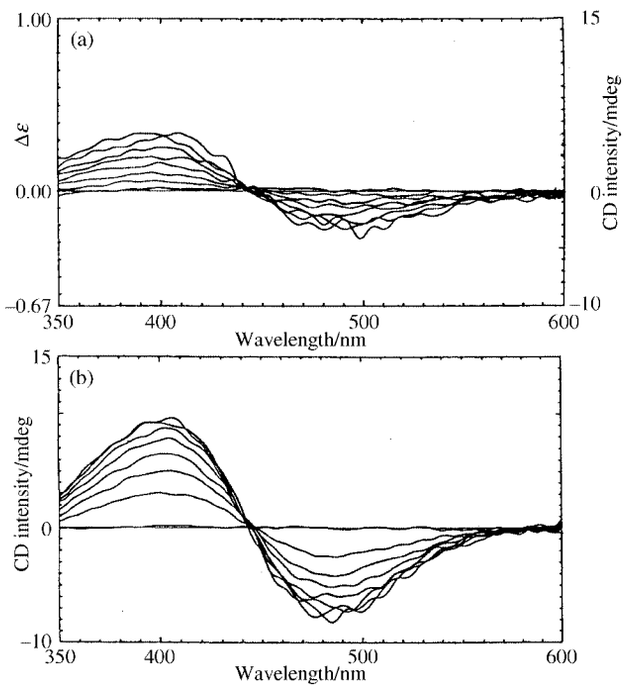

Fig. 4 CD titration of *La* with Fe^{3+} in a) MeOH and b) DMSO. [*La*] = 0.45 mM, [2,6-lutidine] = 2.7 mM, [Fe^{3+}] = 0–0.62 mM.

respectively. The CD band is slightly unsymmetrical due to the cancellation effect of the nearby lying CD band or possibly due to the presence of an unidentified CD band in this region. Furthermore, an observation that the CD intensities are remarkably different in DMSO and MeOH, *i.e.*, much stronger in DMSO than in MeOH, strongly implies that there is a larger difference in configurational energies between two Δ- and Λ-helicates at equilibrium in DMSO *vs.* MeOH.

In Fig. 5 are collected several plots of CD intensities *vs.* Fe^{3+} concentrations in a range of solvents. The fact that the *La* complex shows a negative exciton coupling indicates that the complex adopts predominantly a Δ-helix in all the solvents examined. The amplitudes of the signals at a selected wavelength are summarized in Table 1 together with UV–vis data. The absolute magnitude of the signals with aprotic solvents increased in the order: THF ≤ MeCN < Me_2CO < $HCONH_2$ < DMF < DMSO, indicative of the importance of their hydrogen-bond accepting properties (*β*-values) rather than their overall solvent polarity such as ET and $(\varepsilon - 1)/(2\varepsilon + 1)$ values.[13] This observation strongly suggests that both amido NH and exocyclic NH groups in the *La*–Fe^{3+} complex should

Table 1 UV–vis and CD data for the *La*– and *Lb*–Fe^{3+} complexes in various solvents

	La		*Lb*	
Solvent	λ_{max} (Abs)/nm	CD intensity[a]/mdeg	λ_{max} (Abs)/nm	CD intensity[a]/mdeg
DMSO	462.0 (1.51)	−7.65	469.0 (1.59)	13.1
DMF	462.0 (1.53)	−5.0	467.0 (1.60)	10.0
$HCONH_2$	463.5 (1.39)	−4.5	469.5 (1.45)	7.1
THF	461.0 (1.35)	−0.45	467.0 (1.40)	4.6
MeCN	458.5 (1.41)	−0.72	458.5 (1.44)	3.0
Me_2CO	459.5 (1.44)	−1.25	459.5 (1.50)	1.0
H_2O	456.0 (1.38)	−0.41	462.5 (1.49)	0.0
BuOH	460.0 (1.39)	−0.78	463.5 (1.45)	1.8
EtOH	458.5 (1.42)	−3.10	463.0 (1.46)	−1.8
MeOH	458.0 (1.39)	−3.80	460.0 (1.43)	−2.5

[a] At 480 nm.

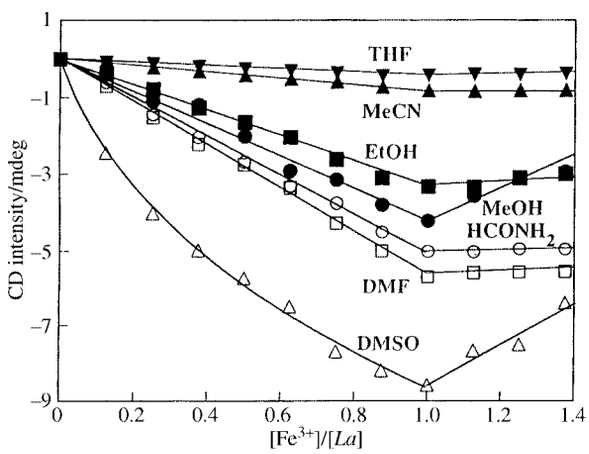

Fig. 5 Variations of CD intensities at 480 nm as a function of [Fe^{3+}]/[*La*] in various solvents. [*La*] = 0.45 mM, [2,6-lutidine] = 2.7 mM, [Fe^{3+}] = 0–0.62 mM.

protrude from the cavity so as to be capable of hydrogen-bonding to the bulk solvents. Particularly, the exocyclic NH groups, as consideration of space-filling CPK molecular models suggests, are unable to enter into the cavity owing to steric crowding in its inner space. In order to give insight into the mechanism of the observed solvent effects on the expression of the helicity, Fig. 6 displays schematic illustrations of the parts of the *La*–Fe^{3+} complexes in the Δ- and Λ-states; the spacer methylenes and the linker amido group are less restricted to rotational freedom for the Δ-triple stranded helicate than for the Λ-helicate; namely, the Δ-helicate has an extended, less sterically congested, and thereby entropically favorable structure, supporting the proposal that the 1-pyrimidinone complex with a negative exciton coupling has Δ-configuration, as does the naturally occurring siderophore enterobactin. Incidentally, CD signals observed in the case of hydroxylic solvents including water are relatively weak in spite of their strong hydrogen-bond accepting ability, where the same helical propensity is still retained. This unequivocally implies that the strong hydrogen-bond accepting abilities of the hydroxylic solvents appear to be almost cancelled by their hydrogen-bond donating abilities.

Complexation of *Lb* with Fe^{3+}

As Fig. 7 shows, the ligand *Lb* exhibited the same stoichiometric behavior as did *La* to form a *Lb*–Fe^{3+} 1:1 complex, which was 25-fold less stable toward removal of Fe^{3+} by EDTA than the *La* complex due probably to an entropic reason (Fig. 8).

The CD spectra of the *Lb* complex are of particular interest

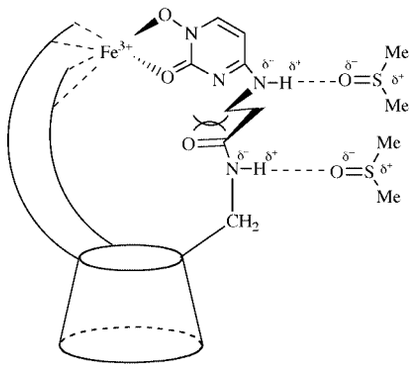

Λ-configuration around the Fe^{3+} ion

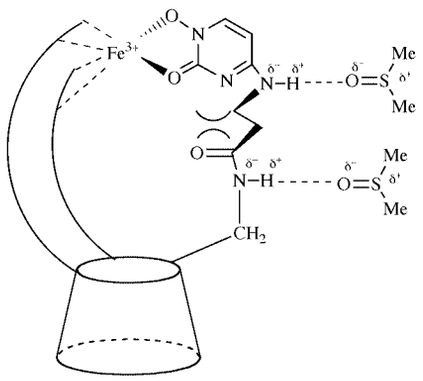

Δ-configuration around the Fe^{3+} ion

Fig. 6 Schematic representation of favorable induction of a Δ- over Λ-helicity around Fe^{3+} in the *La*–Fe^{3+} complex. For simplicity only one of the three side chains is shown. The delta (δ) denotes presumable charge separation.

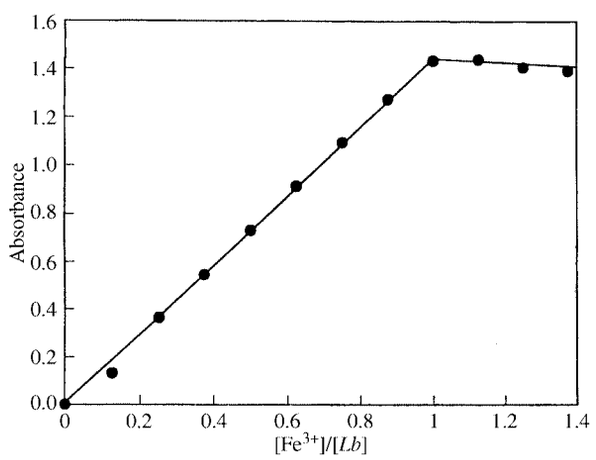

Fig. 7 Variation of UV–vis absorbance at 460 nm as a function of $[Fe^{3+}]/[Lb]$ in MeOH. $[Lb] = 0.3$ mM, [2,6-lutidine] = 1.8 mM, $[Fe^{3+}] = 0$–0.41 mM.

for comparison of its performance with the *La* complex. The CD data are summarized in Fig. 10 and Table 1. The *Lb* complex in highly polar aprotic solvents such as DMF and DMSO exhibited an unexpectedly strong positive exciton coupling with a crossover at 435 nm (Fig. 9b), in spite of its bearing long pentamethylene spacers with high conformational flexibility at the periphery of the coordination site. The positive exciton coupling implies a complexation with a Λ-helix with the same handedness as that for the naturally occurring ferrichrome. On the other hand, MeOH and EtOH provided only a weak negative exciton coupling (Fig. 9a), and water no exciton coupling. In Fig. 11 are given plots of CD intensities *versus* the hydrogen-bond accepting properties (β-values) of the solvent.[13] The approximate linearity within aprotic solvents suggests that

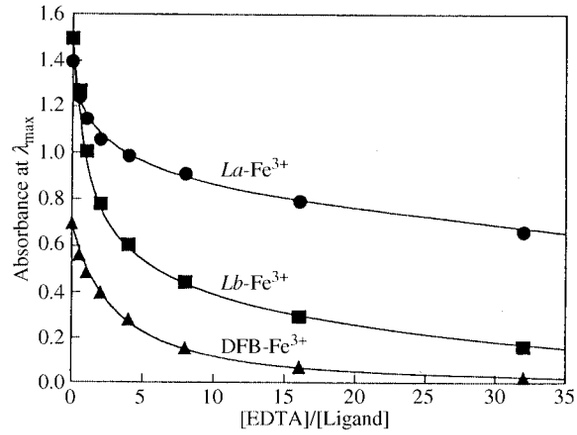

Fig. 8 Comparison of competitive Fe^{3+}-removal by EDTA from the *La*–, *Lb*–, and DFB–Fe^{3+} complexes in MeOH. $[La] = [Lb] = [DFB] = [Fe^{3+}] = 0.3$ mM, [2,6-lutidine] = 2.7 mM, [EDTA] = 0–9.6 mM. DFB: desferrioxamine B.

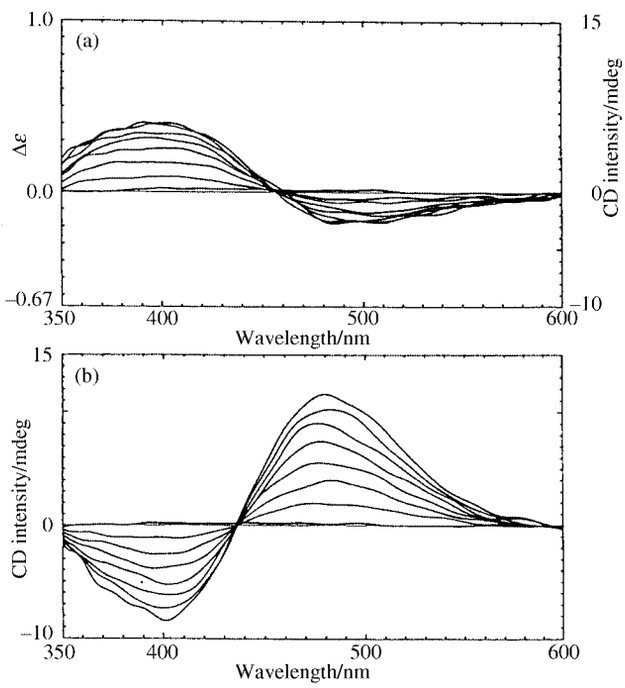

Fig. 9 CD titration of *Lb* with Fe^{3+} in a) MeOH and b) DMSO. $[Lb] = 0.45$ mM, [2,6-lutidine] = 2.7 mM, $[Fe^{3+}] = 0$–0.62 mM.

the induced helicity primarily arises from hydrogen-bonding between the solvent and the amido N–H group rather than the solvent and the amide C=O group (Fig. 11).

Furthermore, it should be noted that the amplitudes of the CD spectra of the *Lb* complex in aprotic solvents were even larger than those of the corresponding *La* complex, although, as CPK models show, all the segments in the side-chains can rotate freely with no inherent barriers; such rotations seem not advantageous for any chiral induction.

Careful inspection of the CPK models reveals that a co-operative combination of two different hydrogen-bonds would prevail in constructing an overall structure of the side chain leading to a large CD amplitude; as illustrated in Fig. 12, the linker amido N–H group is forced to protrude from the inner cavity by a hydrogen-bonding interaction with a bulk solvent molecule (a), while the linker amido carbonyl group is oriented to the inner space of the cavity to form a hydrogen-bond with the exocyclic amino N–H group within the same chain (b). The hydrogen-bond between the exocyclic N–H and amido C=O groups is more preferred in the Λ-helicate than in the Δ-helicate, because the H···O–C hydrogen-bond angle of

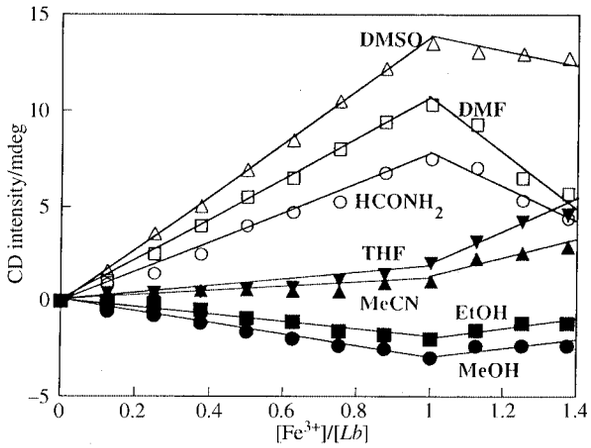

Fig. 10 Variations of CD intensities at 480 nm as a function of $[Fe^{3+}]/[Lb]$ in various solvents. $[Lb] = 0.45$ mM, [2,6-lutidine] = 2.7 mM, $[Fe^{3+}] = 0$–0.62 mM.

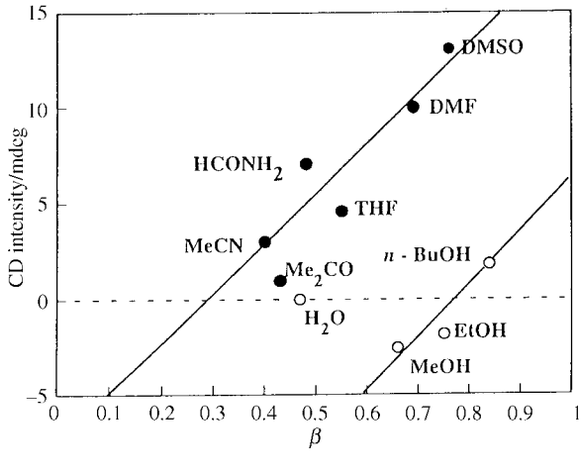

Fig. 11 Plots of CD intensities of the *Lb* complex at 480 nm *versus* β values, which are the hydrogen-bond accepting abilities of the solvents. The line is arbitrarily drawn within aprotic solvents (open circles).

120–150° in the Λ-helix is more favorable than that of less than 90° in the Δ-helix. Conveniently, the hydrogen-bonds thus formed would be largely stabilized by π-electron resonance between the exocyclic amino-nitrogen lone-pair and the electron-withdrawing pyrimidinone group (Scheme 2), and

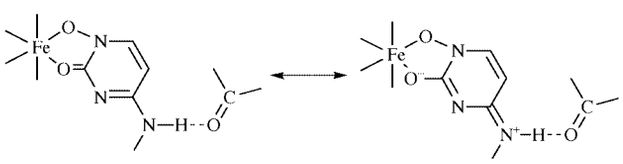

Scheme 2

thereby would direct the side-chain configuration towards a rigid propeller-like arrangement; namely, the enhanced helical propensity in aprotic solvents appears to be attributable in part to the stabilized intramolecular hydrogen-bond and in part to lack of a solvent molecule competing for the exocyclic amino NH groups located in the hydrophobic inner space. Shanzer and his co-workers suggested the importance of formation of extended hydrogen-bond networks in an iron complex; these hydrogen-bonds restrict the conformations to affect the relative stability of the diastereomers and to stabilize the complex once formed.[14] However, such a helical structure would be easily disrupted when the intramolecular hydrogen-bonds are cleaved by a hydroxylic solvent. Actually, no exciton coupling was observed in water. Usually, exciton couplings in alcohols are only small, and negative in MeOH and EtOH but positive in *n*-BuOH, demonstrating that the configuration preferentially adopted by the *Lb*–Fe^{3+} complex depends on the alcoholic solvents employed. Thus, the screw sense of the *Lb* complex in alcohols is somewhat difficult to implicate owing to the complexing nature of hydroxylic solvents. Further study would be needed to explain the cause of the configurational preference for a Δ-helix in MeOH, and for a Λ-helix in *n*-BuOH.

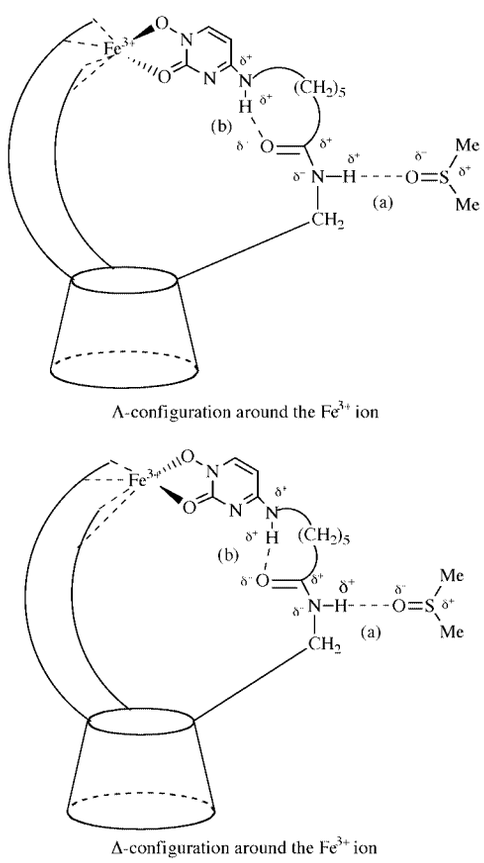

Fig. 12 Schematic representation of favorable induction of a Λ- over Δ-helicity around Fe^{3+} in the *Lb*–Fe^{3+} complex. For simplicity only one of the three side chains is shown. The delta (δ) denotes presumable charge separation.

Conclusions

α-CyD-based, C_3-symmetric, and tripodal ferrichrome mimics with different spacers were prepared and their spectroscopic behavior was examined to investigate the causes of induced helicities. *La* having short spacers exhibited a negative exciton coupling, showing a Δ-helicity in all solvents tested, while *Lb* having long spacers formed a Λ-helicate with an unexpectedly high chirality in highly aprotic solvents such as DMSO and DMF. It became evident that the flexibility of the side chains determines the helicity of the former complex, while intramolecular hydrogen-bonding is substantial for helical induction in the latter complex.

References

1 K. N. Raymond and J. R. Telford, Siderophore-Mediated Iron Transport in Microbes, in *Bioinorganic Chemistry*, ed. D. P. Kessissoglou, Dordrecht Kluwer, 1995, p. 225; K. N. Raymond, G. Mueller and B. F. Matzanke, *Top. Curr. Chem.*, 1984, **123**, 49.

2 J. B. Neilands, T. Peterson and S. A. Leong, High Affinity Iron Transport in Microorganisms, in *Inorganic Chemistry in Biology and Medicines*, ed. A. E. Martell, American Chemical Society, Washington, DC, 1980, p. 263; C. G. Pitt and A. E. Martell, The Design of Chelating Agents for the Treatment of Iron Overload, *ibid.*, p. 279; Y. Sun and A. E. Martell, *The Development of Iron Chelators for Clinical Use*, ed. R. J. Bergeron and G. M. Brittenham, CRC Press, Boca Raton, 1992, p. 345.

3 Y. Tor, J. Libman and A. Shanzer, *J. Am. Chem. Soc.*, 1987, **109**, 6518; A. Shanzer, J. Libman, R. Lazar, Y. Tor and T. Emery, *Biochem. Biophys. Res. Commun.*, 1988, **157**, 389; E. Jurkevitch, Y. Hadar, Y. Chen, J. Libman and A. Shanzer, *J. Bacteriol.*, 1992, **174**, 78; M. Akiyama, A. Katoh, J. Kato, K. Takahashi and K. Hattori, *Chem. Lett.*, 1991, 1189.
4 R. Nudelman, O. Ardon, Y. Hadar, Y. Chen, J. Libman and A. Shanzer, *J. Med. Chem.*, 1998, **41**, 1671; J. Ohkanda and A. Katoh, *Rev. Heteroatom Chem.*, 1998, **18**, 87.
5 Y. Hori, J. Hayashi and S. Tamagaki, *J. Chem. Soc.*, *Chem. Ind. Chem.*, 1998, 417.
6 Y. Hori and S. Tamagaki, *J. Chem. Soc.*, *Chem. Ind. Chem.*, 1998, 602.
7 J. Ohkanda, T. Tokumitsu, K. Mitsuhashi and A. Katoh, *Bull. Chem. Soc. Jpn.*, 1993, **66**, 841; Y. Hida, T. Konakahara and A. Katoh, *J. Org. Chem.*, 1997, **62**, 3618.
8 K. P. Meurer and F. Voegtle, *Top. Curr. Chem.*, 1985, 1; I. W. Zarges, J. Hall, J.-M. Lehn and C. Bolm, *Helv. Chim. Acta*, 1991, **74**, 1843; J. H. Brewster, *Top. Curr. Chem.*, 1974, **47**, 29; C. R. Woods, M. Benaglia, F. Cozzi and J. S. Siegel, *Angew. Chem.*, *Int. Ed. Engl.*, 1996, **35**, 1830.
9 J. Ohkanda, J. Kamitani, T. Tokumitsu, Y. Hida, T. Konakahara and A. Katoh, *J. Org. Chem.*, 1997, **62**, 3618.
10 M. R. Harden, L. J. Jennings and A. Parkin, *J. Chem. Soc.*, *Perkin Trans. 1*, 1990, 2175; W. Klotzer, *Monatsh. Chem.*, 1964, **95**, 1729.
11 S. L. Legen, S. Quici and M. D. Ryan, *J. Am. Chem. Soc.*, 1979, **101**, 7630.
12 S. Blanc, P. Yakirevitch, E. Leize, M. Meyer, J. Libman, A. V. Dorsselaer, A. M. Albrecht and A. Shanzer, *J. Am. Chem. Soc.*, 1997, **119**, 4934.
13 Y. Marcus, *Chem. Soc. Rev.*, 1993, 410.
14 J. Libman and Y. Tor, *J. Am. Chem. Soc.*, 1987, **109**, 5880; A. Shanzer, J. Libman and S. Lifson, *Pure Appl. Chem.*, 1992, **64**, 1421; I. Dayan, J. Libman, Y. Agi and A. Shanzer, *Inorg. Chem.*, 1993, **32**, 1467.

Paper a904153b